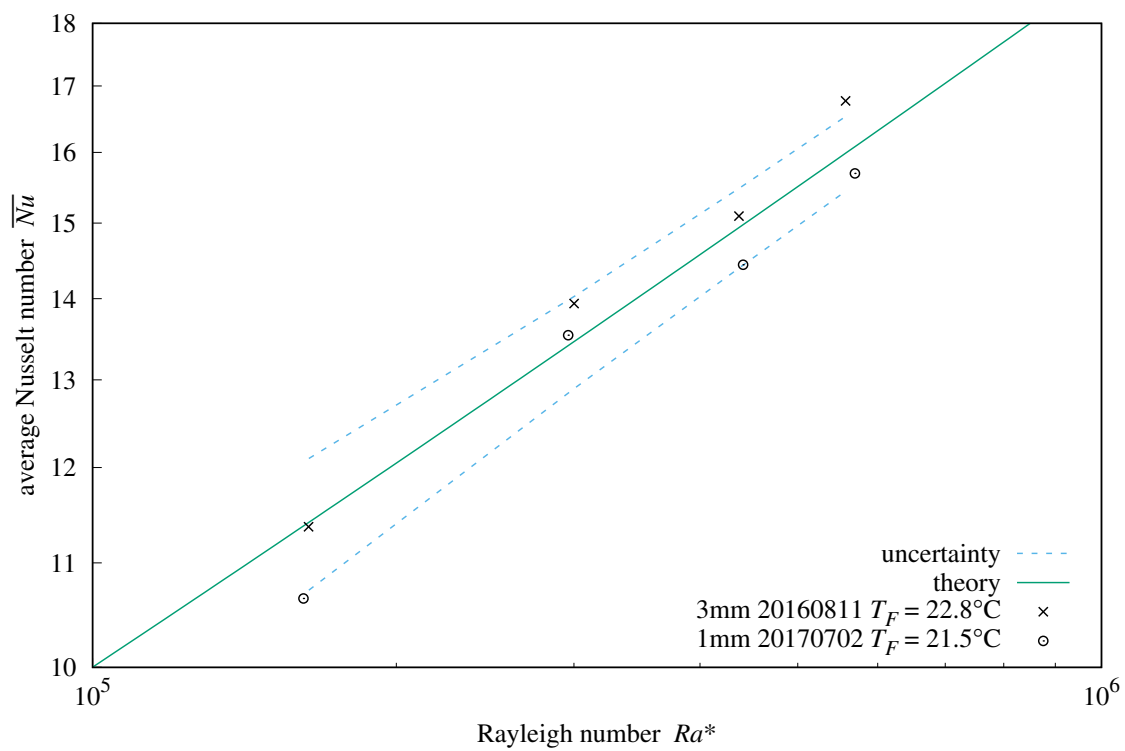
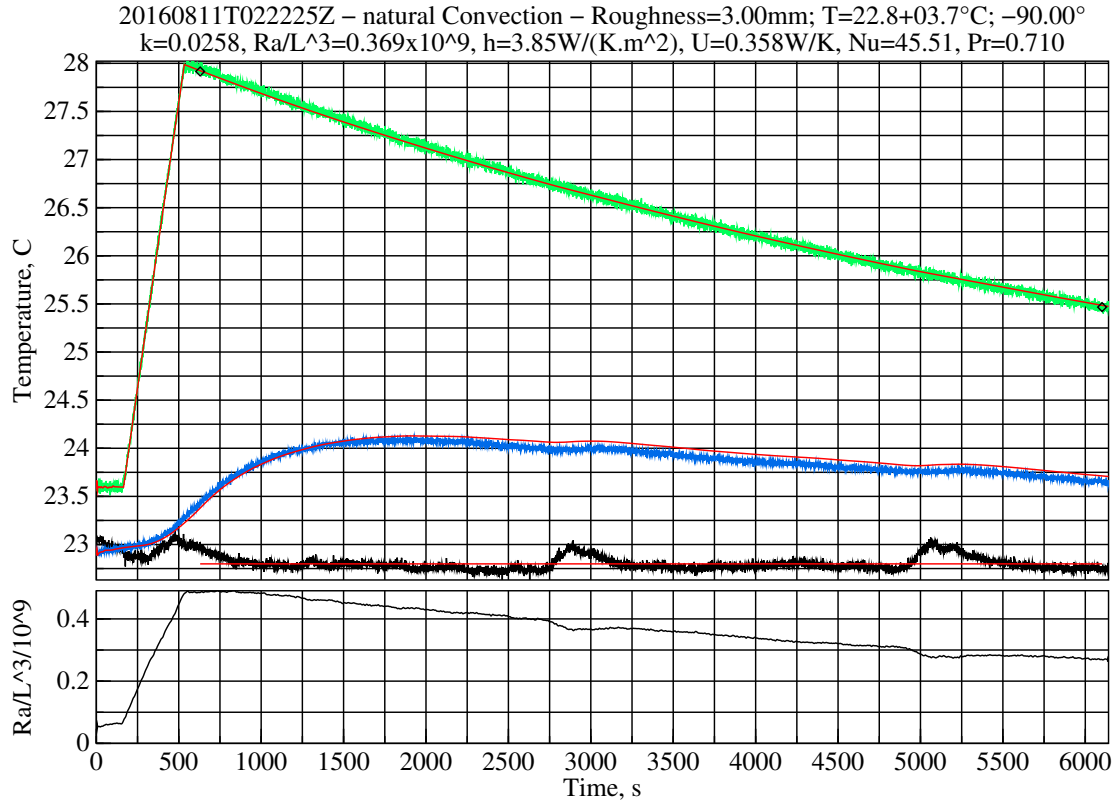


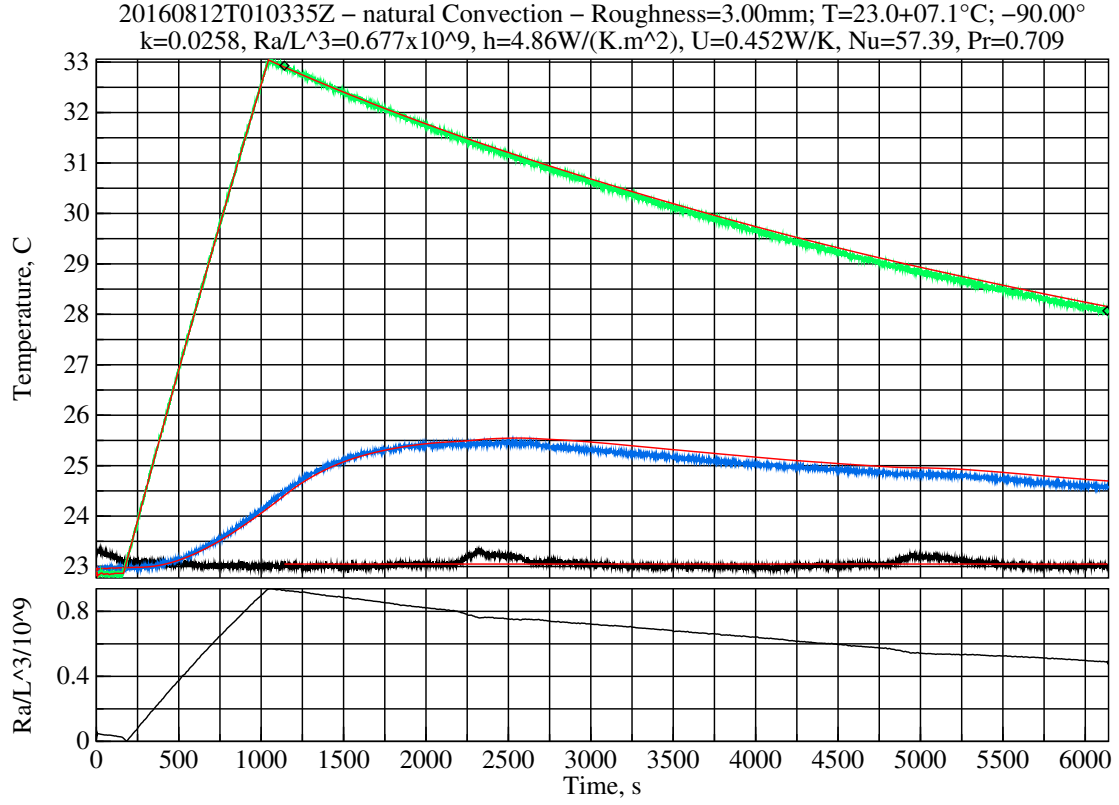
Upward natural convection





Estimated measurement uncertainties of natural convection at $\theta = -90.0$.

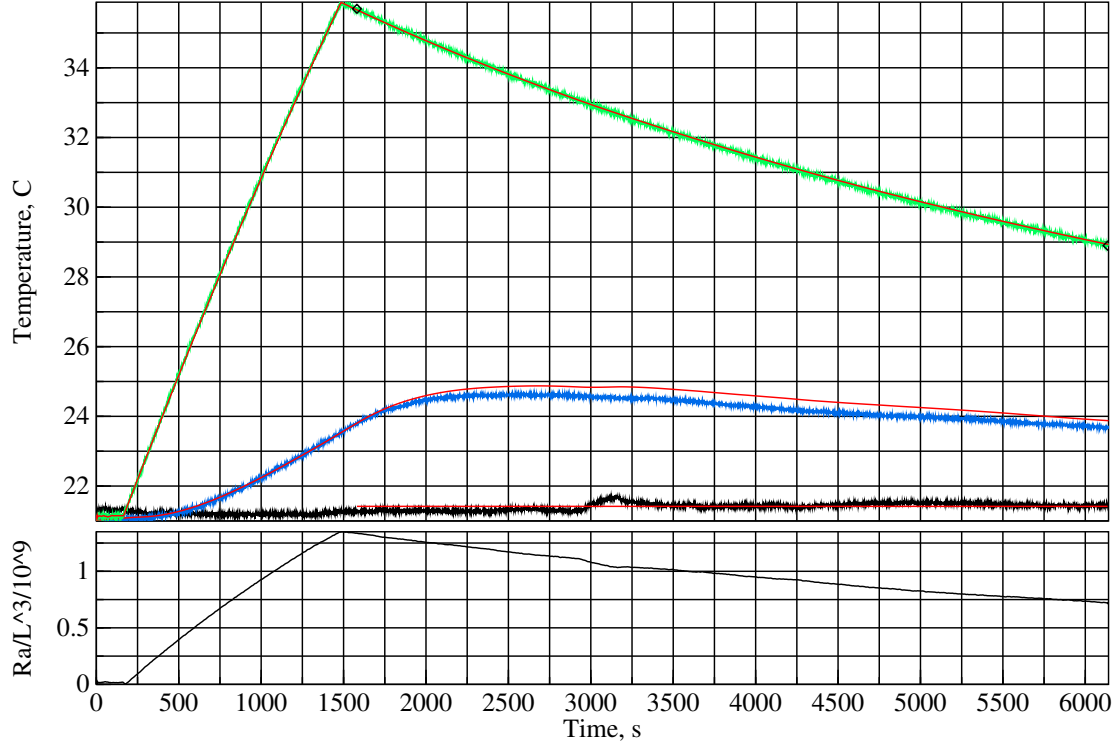
Symbol	Nominal	Sensitivity	Bias	Uncertainty	Component
ΔT	3.75K	+46.4%/K	0.10K	4.64%	LM35C differential
P	101kPa	+0.0005%/Pa	1.5kPa	0.75%	MPXH6115A6U air pressure
C_{pt}	4.69kJ/K	+0.032%/(J/K)	47J/K	1.49%	plate thermal capacity
C_S	1.000	–41.2%	0.050	2.06%	side reuptake
C_B	1.000	–13.6%	0.100	1.36%	back reuptake
L_c	0.305m	+456%/m	500um	0.23%	characteristic length
L_m	3.57mm	+1040%/m	500um	0.52%	side metal strip width
ϵ_{XPS}	0.515	+33.2%	0.010	0.33%	XPS emissivity
ϵ_{tp}	0.890	+39.9%	0.015	0.60%	tape emissivity
Ω_{tp}	0.540	+27.0%	0.020	0.54%	tape coverage
ϵ_{rs}	0.040	+140%	0.010	1.40%	test-surface emissivity
ϵ_{wt}	0.900	+64.6%	0.025	1.62%	wind-tunnel emissivity
				6.00%	combined bias uncertainty



Estimated measurement uncertainties of natural convection at $\theta = -90.0$.

Symbol	Nominal	Sensitivity	Bias	Uncertainty	Component
ΔT	7.10K	+23.5%/K	0.10K	2.35%	LM35C differential
P	101kPa	+0.0005%/Pa	1.5kPa	0.77%	MPXH6115A6U air pressure
C_{pt}	4.69kJ/K	+0.030%/(J/K)	47J/K	1.41%	plate thermal capacity
C_S	1.000	–39.7%	0.050	1.98%	side reuptake
C_B	1.000	–11.7%	0.100	1.17%	back reuptake
L_c	0.305m	+433%/m	500um	0.22%	characteristic length
L_m	3.57mm	+906%/m	500um	0.45%	side metal strip width
ϵ_{XPS}	0.515	+28.1%	0.010	0.28%	XPS emissivity
ϵ_{tp}	0.890	+33.8%	0.015	0.51%	tape emissivity
Ω_{tp}	0.540	+22.9%	0.020	0.46%	tape coverage
ϵ_{rs}	0.040	+120%	0.010	1.20%	test-surface emissivity
ϵ_{wt}	0.900	+54.9%	0.025	1.37%	wind-tunnel emissivity
				4.19%	combined bias uncertainty

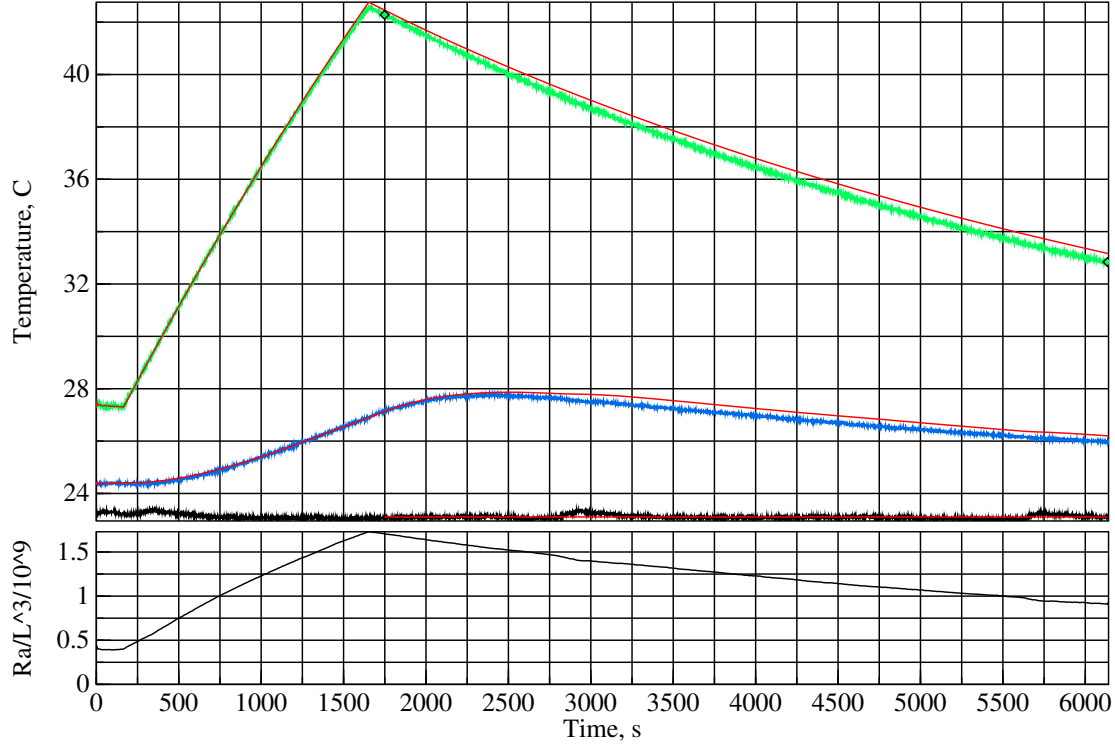
20160812T230328Z – natural Convection – Roughness=3.00mm; T=21.4+10.4°C; –90.00°
k=0.0257, Ra/L^3=0.986x10^9, h=5.10W/(K.m^2), U=0.474W/K, Nu=60.42, Pr=0.709



Estimated measurement uncertainties of natural convection at $\theta = -90.0$.

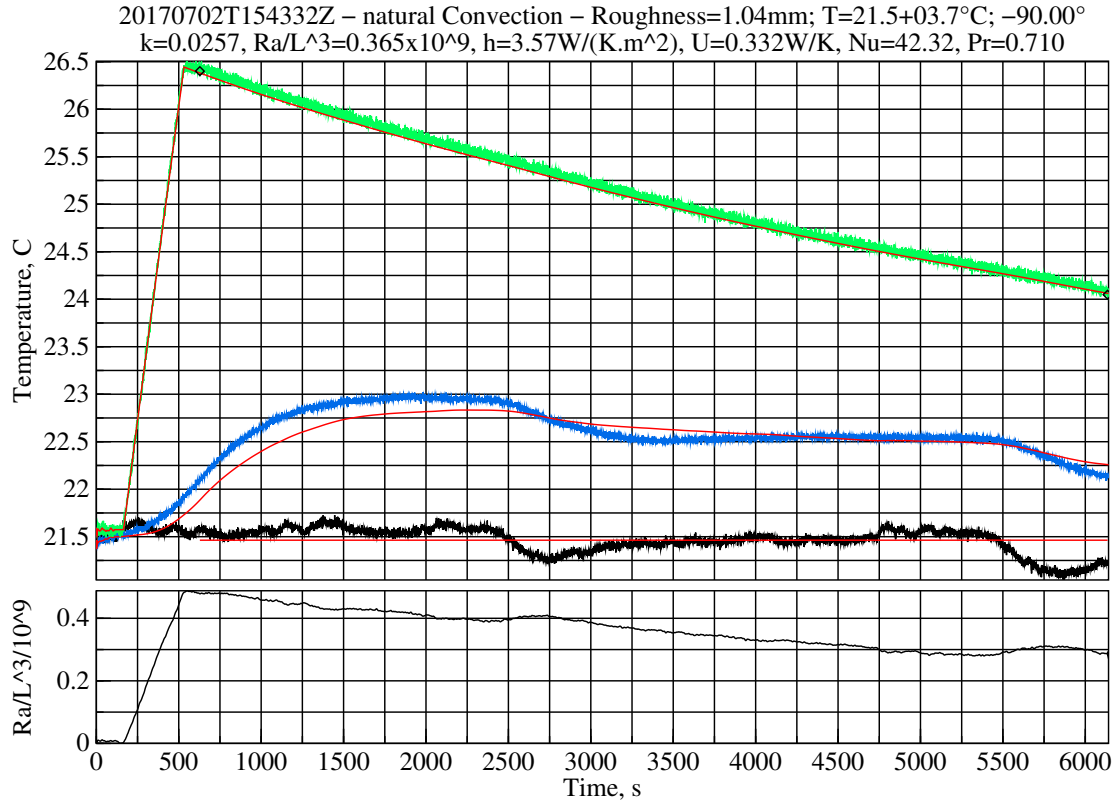
Symbol	Nominal	Sensitivity	Bias	Uncertainty	Component
ΔT	10.4K	+15.6%/K	0.10K	1.56%	LM35C differential
P	100kPa	+0.0005%/Pa	1.5kPa	0.79%	MPXH6115A6U air pressure
C_{pt}	4.69kJ/K	+0.029%/(J/K)	47J/K	1.36%	plate thermal capacity
C_S	1.000	–38.8%	0.050	1.94%	side reuptake
C_B	1.000	–10.7%	0.100	1.07%	back reuptake
L_c	0.305m	+420%/m	500um	0.21%	characteristic length
L_m	3.57mm	+826%/m	500um	0.41%	side metal strip width
ϵ_{XPS}	0.515	+25.0%	0.010	0.25%	XPS emissivity
ϵ_{tp}	0.890	+30.2%	0.015	0.45%	tape emissivity
Ω_{tp}	0.540	+20.4%	0.020	0.41%	tape coverage
ϵ_{rs}	0.040	+109%	0.010	1.09%	test-surface emissivity
ϵ_{wt}	0.900	+49.0%	0.025	1.23%	wind-tunnel emissivity
				3.63%	combined bias uncertainty

20160812T030455Z – natural Convection – Roughness=3.00mm; T=23.1+13.8°C; –90.00°
k=0.0258, Ra/L^3=1.258x10^9, h=5.66W/(K.m^2), U=0.527W/K, Nu=66.86, Pr=0.709



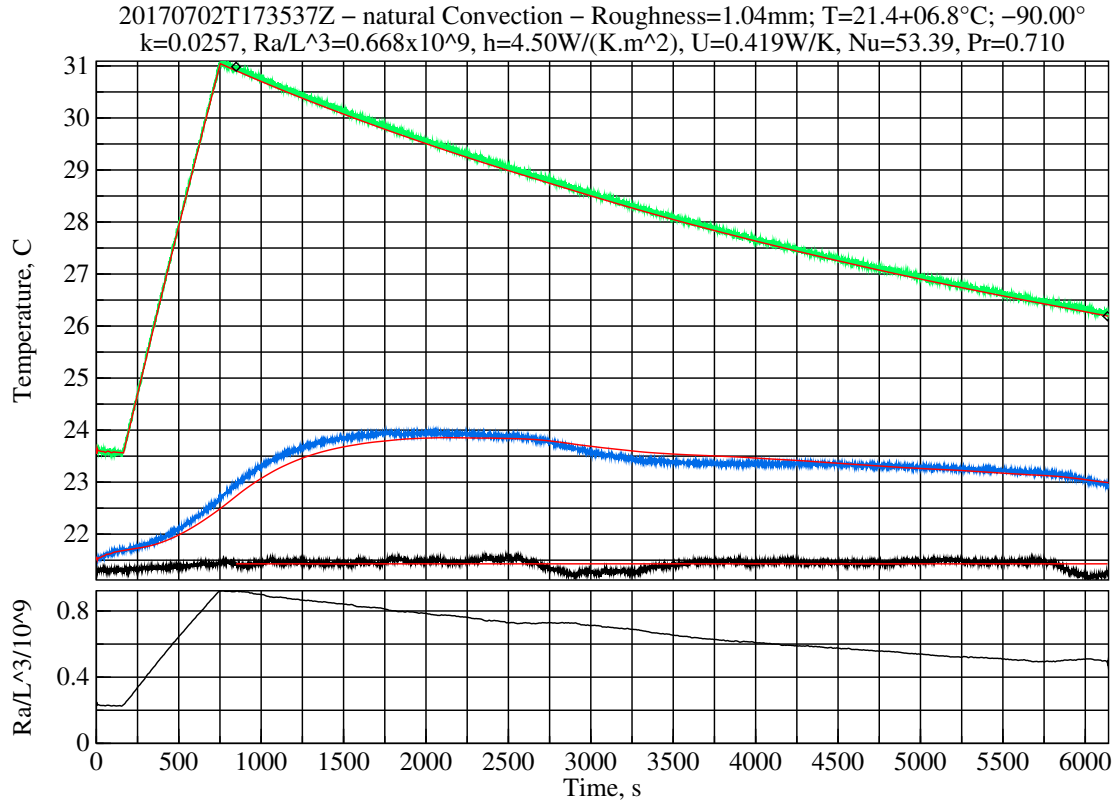
Estimated measurement uncertainties of natural convection at $\theta = -90.0$.

Symbol	Nominal	Sensitivity	Bias	Uncertainty	Component
ΔT	13.8K	+11.7%/K	0.10K	1.17%	LM35C differential
P	101kPa	+0.0005%/Pa	1.5kPa	0.79%	MPXH6115A6U air pressure
C_{pt}	4.69kJ/K	+0.029%/(J/K)	47J/K	1.35%	plate thermal capacity
C_S	1.000	–38.2%	0.050	1.91%	side reuptake
C_B	1.000	–10.1%	0.100	1.01%	back reuptake
L_c	0.305m	+416%/m	500um	0.21%	characteristic length
L_m	3.57mm	+798%/m	500um	0.40%	side metal strip width
ϵ_{XPS}	0.515	+24.0%	0.010	0.24%	XPS emissivity
ϵ_{tp}	0.890	+29.0%	0.015	0.44%	tape emissivity
Ω_{tp}	0.540	+19.6%	0.020	0.39%	tape coverage
ϵ_{rs}	0.040	+105%	0.010	1.05%	test-surface emissivity
ϵ_{wt}	0.900	+47.1%	0.025	1.18%	wind-tunnel emissivity
				3.41%	combined bias uncertainty



Estimated measurement uncertainties of natural convection at $\theta = -90.0$.

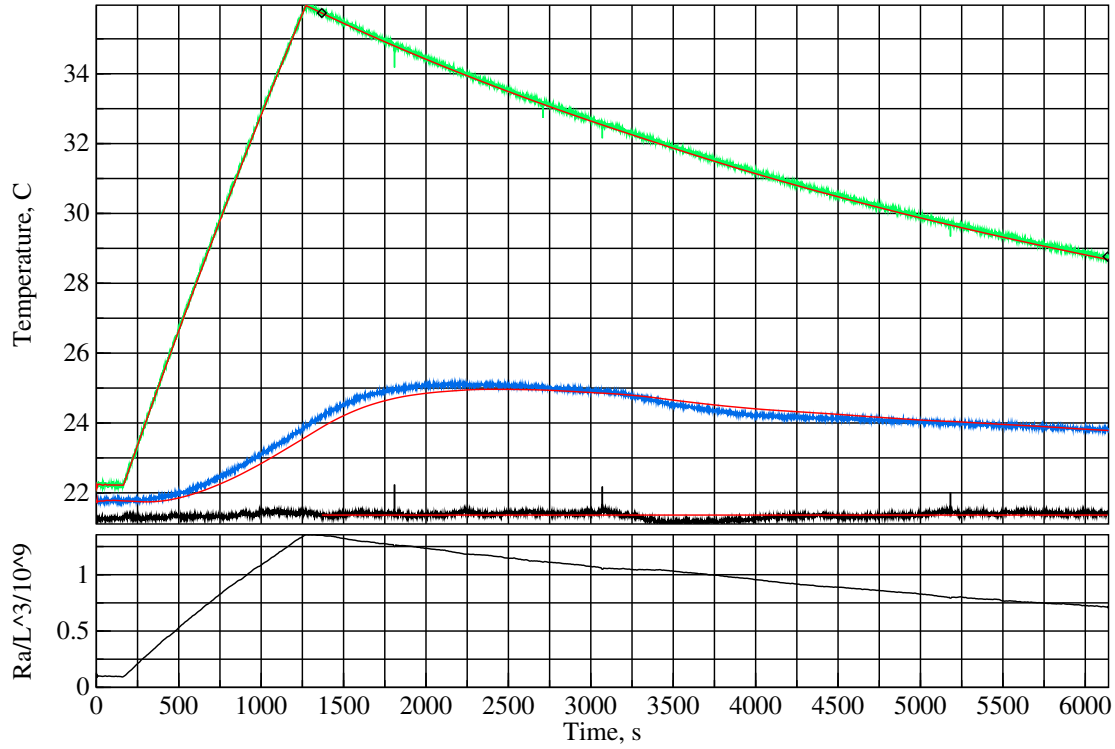
Symbol	Nominal	Sensitivity	Bias	Uncertainty	Component
ΔT	3.66K	+43.4%/K	0.10K	4.34%	LM35C differential
P	101kPa	+0.0005%/Pa	1.5kPa	0.77%	MPXH6115A6U air pressure
C_{pt}	4.24kJ/K	+0.031%/(J/K)	42J/K	1.33%	plate thermal capacity
C_S	1.000	–38.4%	0.050	1.92%	side reuptake
C_B	1.000	–13.7%	0.100	1.37%	back reuptake
L_c	0.305m	+406%/m	500um	0.20%	characteristic length
L_m	3.57mm	+691%/m	500um	0.35%	side metal strip width
ϵ_{XPS}	0.515	+63.1%	0.010	0.63%	XPS emissivity
ϵ_{rs}	0.040	+139%	0.010	1.39%	test-surface emissivity
ϵ_{wt}	0.900	+45.0%	0.025	1.13%	wind-tunnel emissivity
				5.52%	combined bias uncertainty



Estimated measurement uncertainties of natural convection at $\theta = -90.0$.

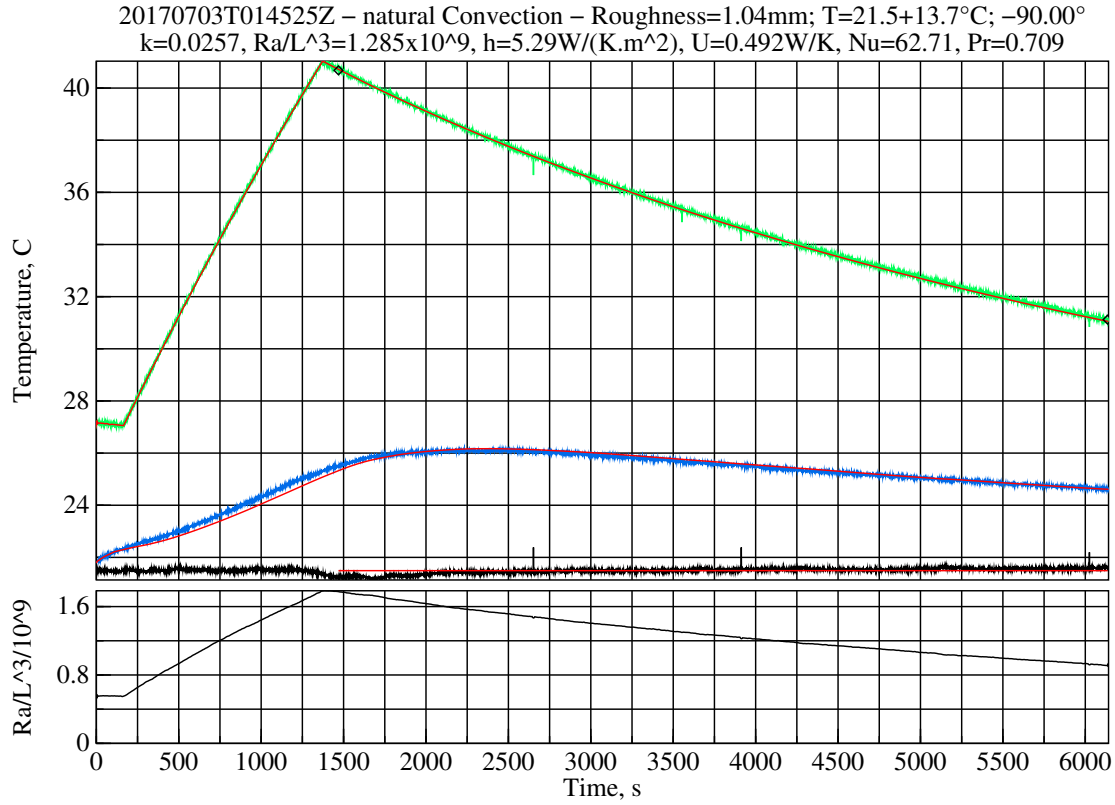
Symbol	Nominal	Sensitivity	Bias	Uncertainty	Component
ΔT	6.84K	+22.5%/K	0.10K	2.25%	LM35C differential
P	101kPa	+0.0005%/Pa	1.5kPa	0.79%	MPXH6115A6U air pressure
C_{pt}	4.24kJ/K	+0.030%/(J/K)	42J/K	1.28%	plate thermal capacity
C_S	1.000	–36.8%	0.050	1.84%	side reuptake
C_B	1.000	–11.8%	0.100	1.18%	back reuptake
L_m	3.57mm	+595%/m	500um	0.30%	side metal strip width
ϵ_{XPS}	0.515	+53.1%	0.010	0.53%	XPS emissivity
ϵ_{rs}	0.040	+119%	0.010	1.19%	test-surface emissivity
ϵ_{wt}	0.900	+38.0%	0.025	0.95%	wind-tunnel emissivity
				3.86%	combined bias uncertainty

20170702T234939Z – natural Convection – Roughness=1.04mm; T=21.4+10.4°C; –90.00°
k=0.0257, Ra/L^3=0.996x10^9, h=4.91W/(K.m^2), U=0.457W/K, Nu=58.31, Pr=0.710



Estimated measurement uncertainties of natural convection at $\theta = -90.0$.

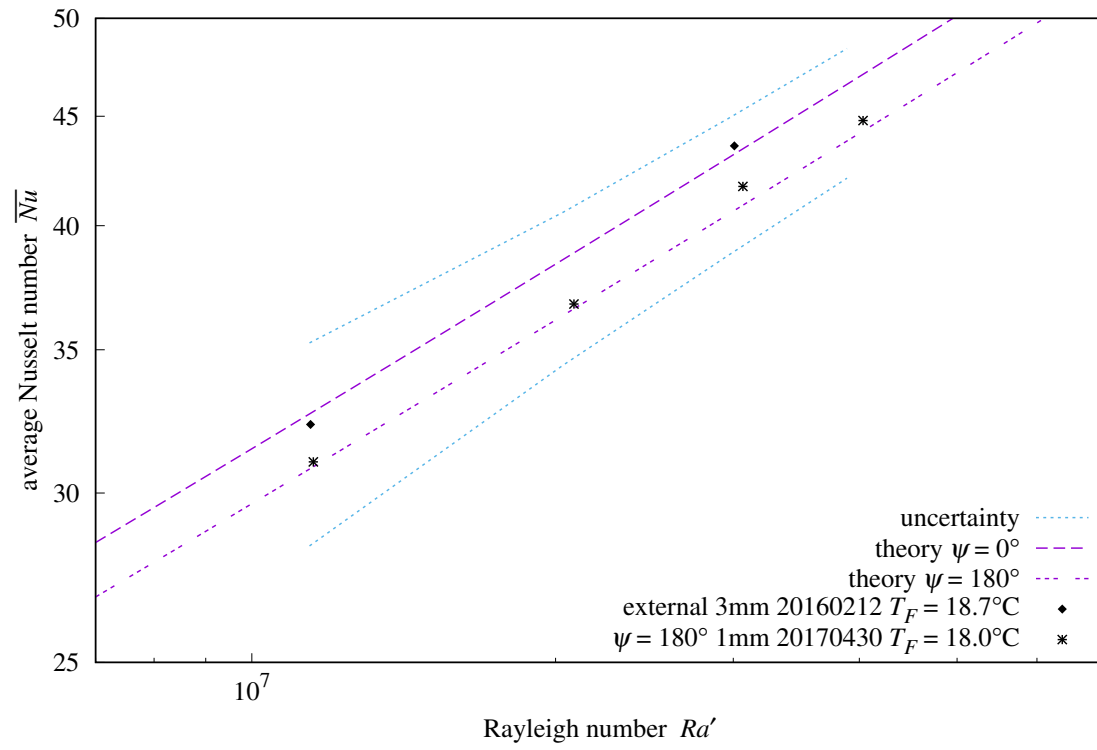
Symbol	Nominal	Sensitivity	Bias	Uncertainty	Component
ΔT	10.4K	+14.6%/K	0.10K	1.46%	LM35C differential
P	101kPa	+0.0005%/Pa	1.5kPa	0.80%	MPXH6115A6U air pressure
C_{pt}	4.24kJ/K	+0.030%/(J/K)	42J/K	1.25%	plate thermal capacity
C_S	1.000	–35.9%	0.050	1.80%	side reuptake
C_B	1.000	–10.7%	0.100	1.07%	back reuptake
L_m	3.57mm	+542%/m	500um	0.27%	side metal strip width
ϵ_{XPS}	0.515	+47.6%	0.010	0.48%	XPS emissivity
ϵ_{rs}	0.040	+109%	0.010	1.09%	test-surface emissivity
ϵ_{wt}	0.900	+34.2%	0.025	0.86%	wind-tunnel emissivity
				3.31%	combined bias uncertainty

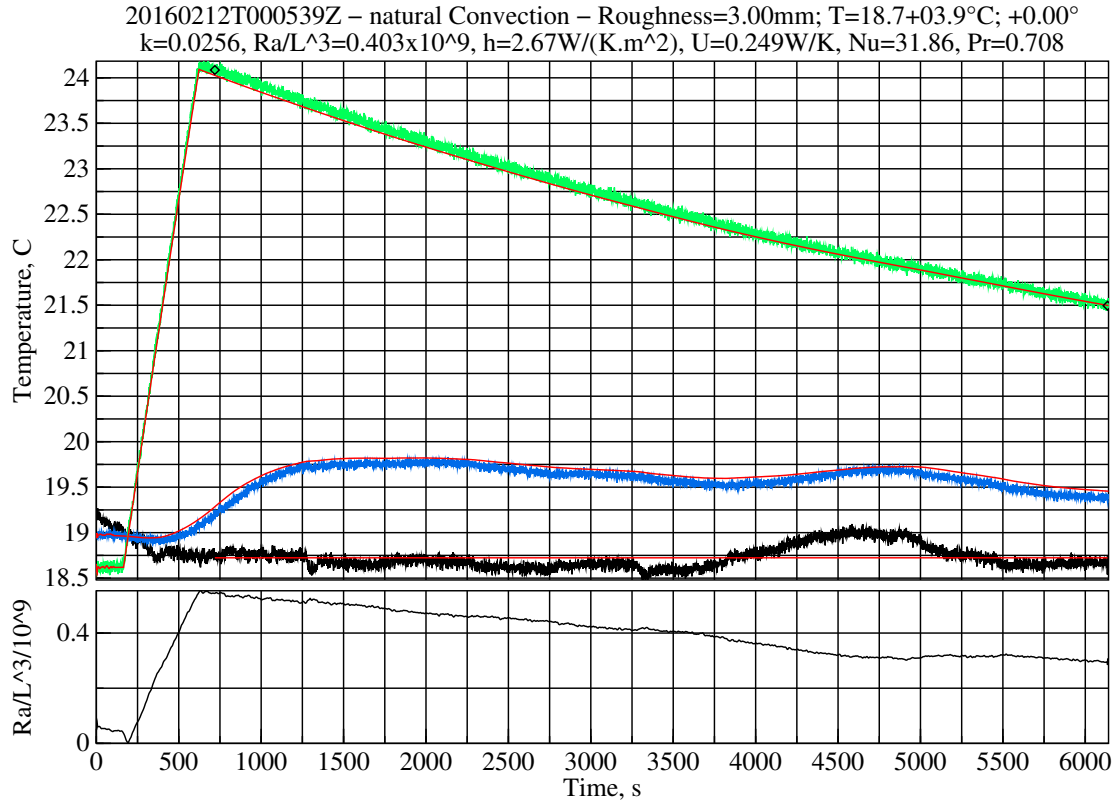


Estimated measurement uncertainties of natural convection at $\theta = -90.0$.

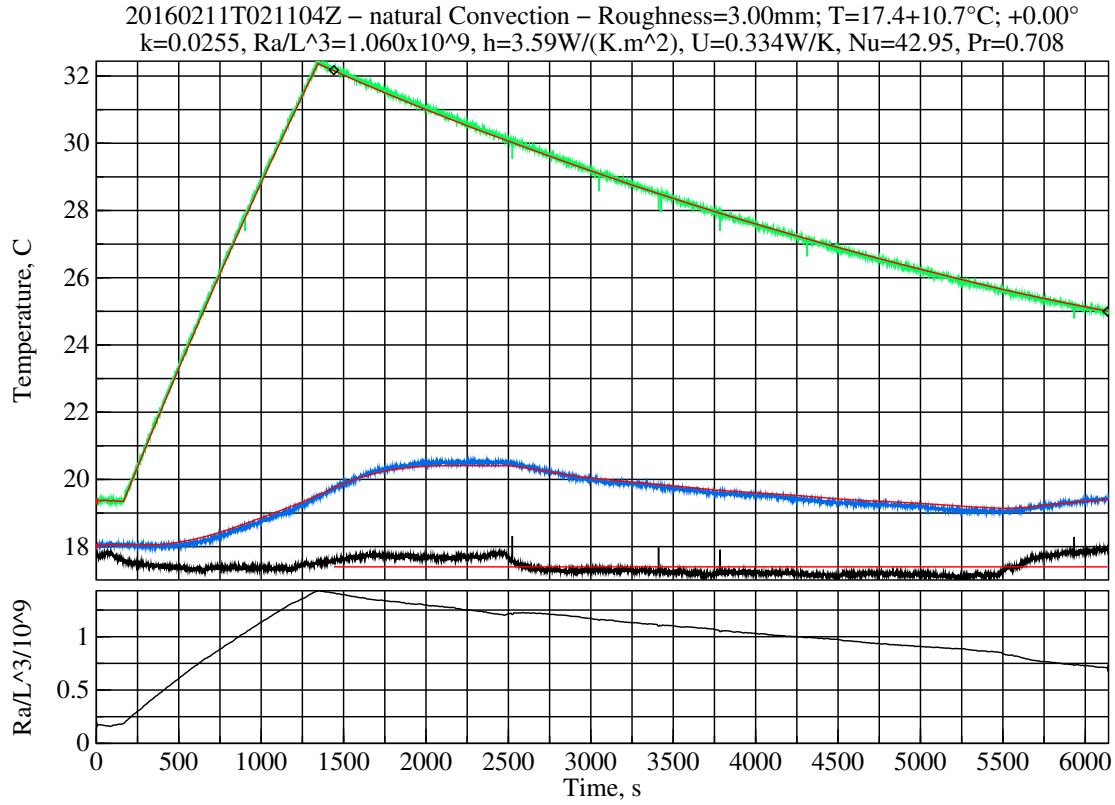
Symbol	Nominal	Sensitivity	Bias	Uncertainty	Component
ΔT	13.7K	+11.0%/K	0.10K	1.10%	LM35C differential
P	101kPa	+0.0005%/Pa	1.5kPa	0.80%	MPXH6115A6U air pressure
C_{pt}	4.24kJ/K	+0.029%/(J/K)	42J/K	1.24%	plate thermal capacity
C_S	1.000	–35.3%	0.050	1.77%	side reuptake
C_B	1.000	–10.0%	0.100	1.00%	back reuptake
L_m	3.57mm	+514%/m	500um	0.26%	side metal strip width
ϵ_{XPS}	0.515	+44.7%	0.010	0.45%	XPS emissivity
ϵ_{rs}	0.040	+103%	0.010	1.03%	test-surface emissivity
ϵ_{wt}	0.900	+32.2%	0.025	0.81%	wind-tunnel emissivity
				3.09%	combined bias uncertainty

Vertical plate natural convection



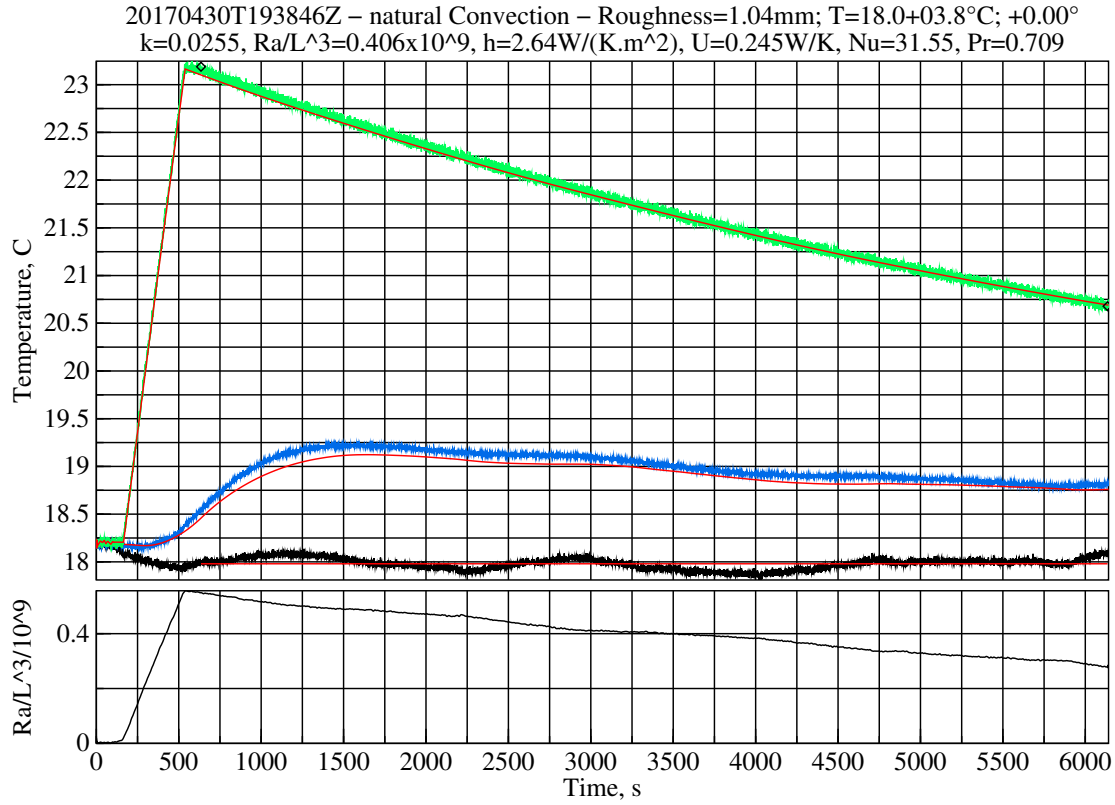


Estimated measurement uncertainties of natural convection at $\theta = 0.0$.					
Symbol	Nominal	Sensitivity	Bias	Uncertainty	Component
ΔT	3.91K	+65.2%/K	0.10K	6.52%	LM35C differential
T_{bb}	292K	+0.416%/K	0.50K	0.21%	radiative temperature
P	100kPa	+0.0007%/Pa	1.5kPa	1.02%	MPXH6115A6U air pressure
C_{pt}	4.69kJ/K	+0.047%/(J/K)	47J/K	2.21%	plate thermal capacity
C_V	1.000	−15.5%	0.100	1.55%	vertical reuptake
L_c	0.305m	+664%/m	500um	0.33%	characteristic length
D_{PIR}	25.4mm	−625%/m	1.0mm	0.63%	insulation thickness
D_g	1.00mm	−634%/m	500um	0.32%	air gap
L_m	3.57mm	+1382%/m	500um	0.69%	side metal strip width
k_{PIR}	22.2 $\frac{mW}{K \cdot m}$	+0.605%/ $\frac{mW}{K \cdot m}$	1.1 $\frac{mW}{K \cdot m}$	0.67%	PIR thermal conductivity
ϵ_{XPS}	0.515	+46.2%	0.010	0.46%	XPS emissivity
ϵ_{tp}	0.890	+55.3%	0.015	0.83%	tape emissivity
Ω_{tp}	0.540	+37.7%	0.020	0.75%	tape coverage
ϵ_{rs}	0.040	+189%	0.010	1.89%	test-surface emissivity
ϵ_{wt}	0.900	+90.9%	0.025	2.27%	wind-tunnel emissivity
				7.92%	combined bias uncertainty

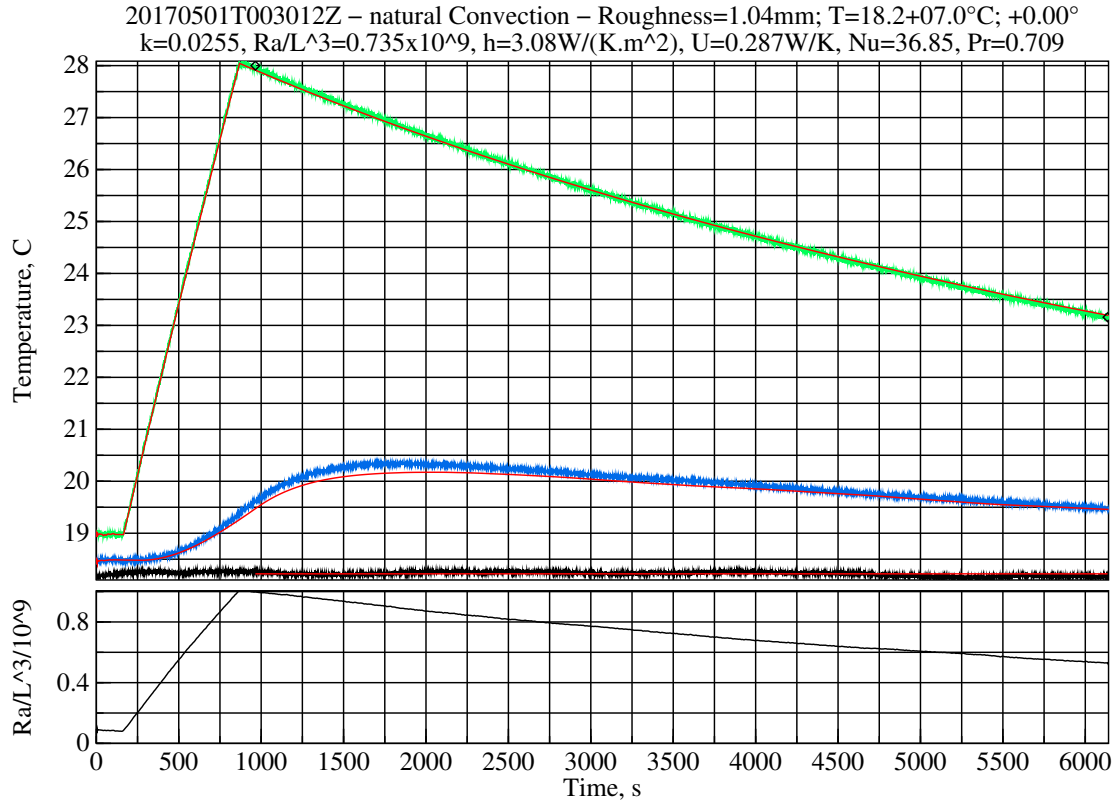


Estimated measurement uncertainties of natural convection at $\theta = 0.0$.

Symbol	Nominal	Sensitivity	Bias	Uncertainty	Component
ΔT	10.7K	+21.7%/K	0.10K	2.17%	LM35C differential
P	99.4kPa	+0.0007%/Pa	1.5kPa	1.05%	MPXH6115A6U air pressure
C_{pt}	4.69kJ/K	+0.042%/(J/K)	47J/K	1.98%	plate thermal capacity
C_V	1.000	−14.2%	0.100	1.42%	vertical reuptake
L_c	0.305m	+598%/m	500um	0.30%	characteristic length
D_{PIR}	25.4mm	−513%/m	1.0mm	0.51%	insulation thickness
D_g	1.00mm	−520%/m	500um	0.26%	air gap
L_m	3.57mm	+1090%/m	500um	0.55%	side metal strip width
k_{PIR}	22.2 $\frac{mW}{K \cdot m}$	+0.496%/ $\frac{mW}{K \cdot m}$	1.1 $\frac{mW}{K \cdot m}$	0.55%	PIR thermal conductivity
ϵ_{XPS}	0.515	+34.8%	0.010	0.35%	XPS emissivity
ϵ_{tp}	0.890	+41.9%	0.015	0.63%	tape emissivity
Ω_{tp}	0.540	+28.4%	0.020	0.57%	tape coverage
ϵ_{rs}	0.040	+147%	0.010	1.47%	test-surface emissivity
ϵ_{wt}	0.900	+68.6%	0.025	1.71%	wind-tunnel emissivity
				4.33%	combined bias uncertainty

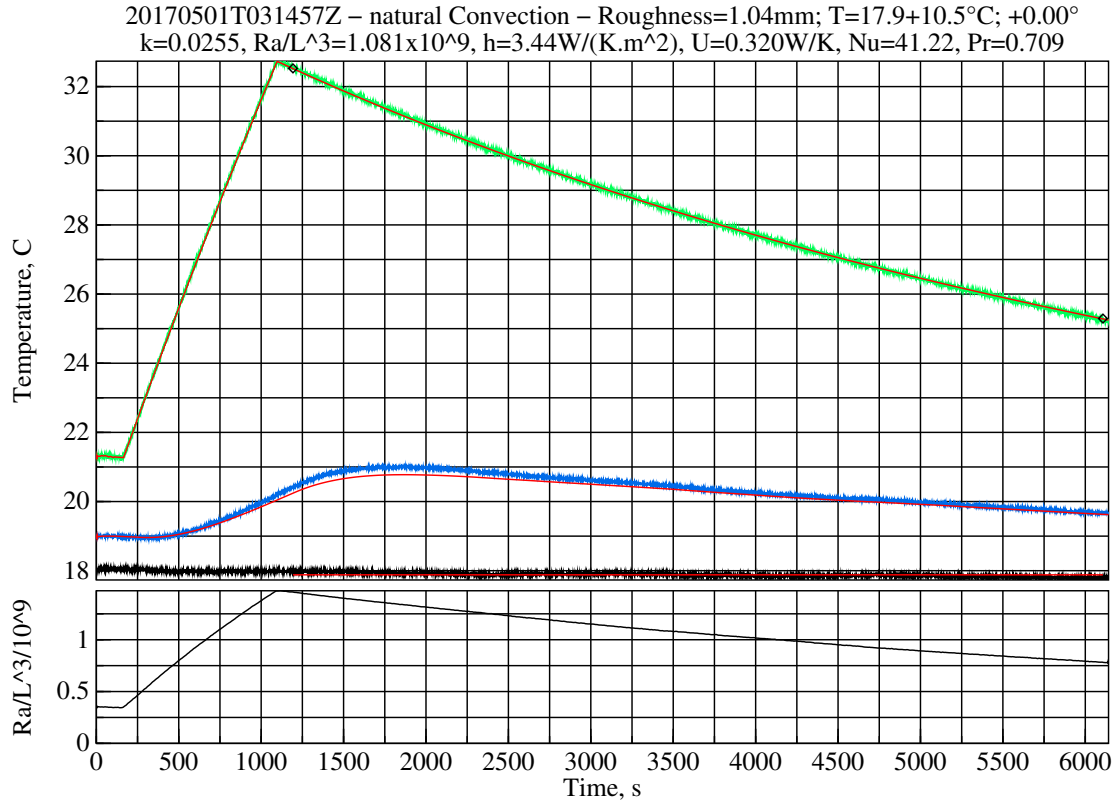


Estimated measurement uncertainties of natural convection at $\theta = 0.0$.					
Symbol	Nominal	Sensitivity	Bias	Uncertainty	Component
ΔT	3.79K	+63.2%/K	0.10K	6.32%	LM35C differential
P	102kPa	+0.0007%/Pa	1.5kPa	1.00%	MPXH6115A6U air pressure
C_{pt}	4.24kJ/K	+0.048%/(J/K)	42J/K	2.05%	plate thermal capacity
C_V	1.000	−15.4%	0.100	1.54%	vertical reuptake
L_c	0.305m	+611%/m	500um	0.31%	characteristic length
D_{PIR}	25.4mm	−652%/m	1.0mm	0.65%	insulation thickness
D_g	1.00mm	−662%/m	500um	0.33%	air gap
L_m	3.57mm	+1357%/m	500um	0.68%	side metal strip width
k_{PIR}	22.2 $\frac{mW}{K \cdot m}$	+0.631%/ $\frac{mW}{K \cdot m}$	1.1 $\frac{mW}{K \cdot m}$	0.70%	PIR thermal conductivity
ϵ_{XPS}	0.515	+47.5%	0.010	0.48%	XPS emissivity
ϵ_{tp}	0.550	+57.0%	0.015	0.86%	tape emissivity
ϵ_{rs}	0.040	+199%	0.010	1.99%	test-surface emissivity
ϵ_{wt}	0.900	+72.5%	0.025	1.81%	wind-tunnel emissivity
				7.58%	combined bias uncertainty



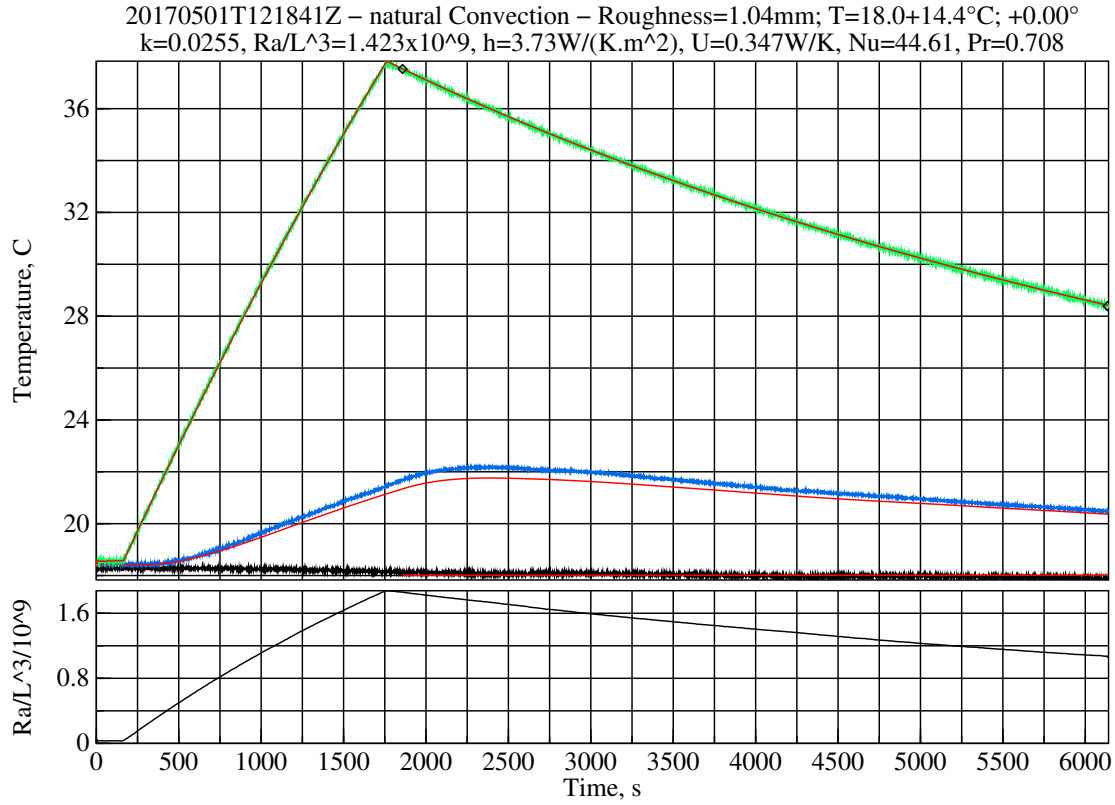
Estimated measurement uncertainties of natural convection at $\theta = 0.0$.

Symbol	Nominal	Sensitivity	Bias	Uncertainty	Component
ΔT	7.03K	+32.3%/K	0.10K	3.23%	LM35C differential
P	102kPa	+0.0007%/Pa	1.5kPa	1.02%	MPXH6115A6U air pressure
C_{pt}	4.24kJ/K	+0.045%/(J/K)	42J/K	1.93%	plate thermal capacity
C_V	1.000	−14.5%	0.100	1.45%	vertical reuptake
L_c	0.305m	+577%/m	500um	0.29%	characteristic length
D_{PIR}	25.4mm	−579%/m	1.0mm	0.58%	insulation thickness
D_g	1.00mm	−587%/m	500um	0.29%	air gap
L_m	3.57mm	+1167%/m	500um	0.58%	side metal strip width
k_{PIR}	22.2 $\frac{\text{mW}}{\text{K} \cdot \text{m}}$	+0.559%/ $\frac{\text{mW}}{\text{K} \cdot \text{m}}$	1.1 $\frac{\text{mW}}{\text{K} \cdot \text{m}}$	0.62%	PIR thermal conductivity
ϵ_{XPS}	0.515	+40.1%	0.010	0.40%	XPS emissivity
ϵ_{tp}	0.550	+48.2%	0.015	0.72%	tape emissivity
ϵ_{rs}	0.040	+171%	0.010	1.71%	test-surface emissivity
ϵ_{wt}	0.900	+61.1%	0.025	1.53%	wind-tunnel emissivity
				4.96%	combined bias uncertainty

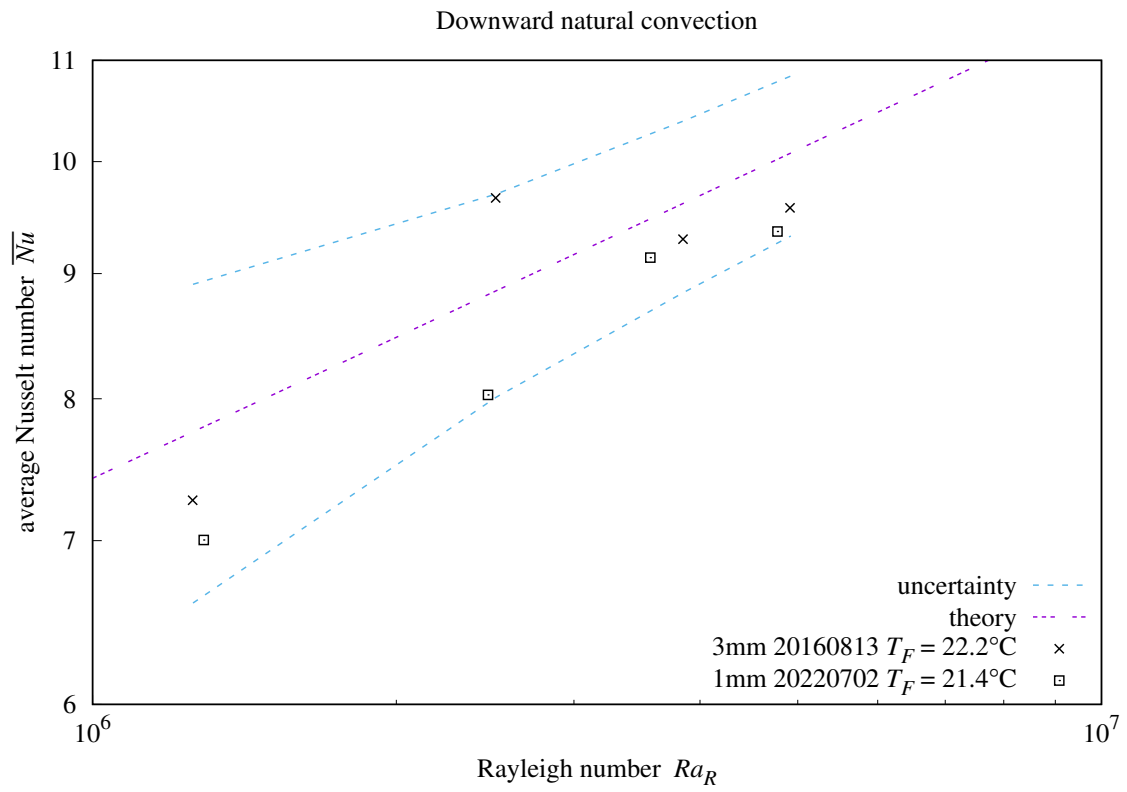


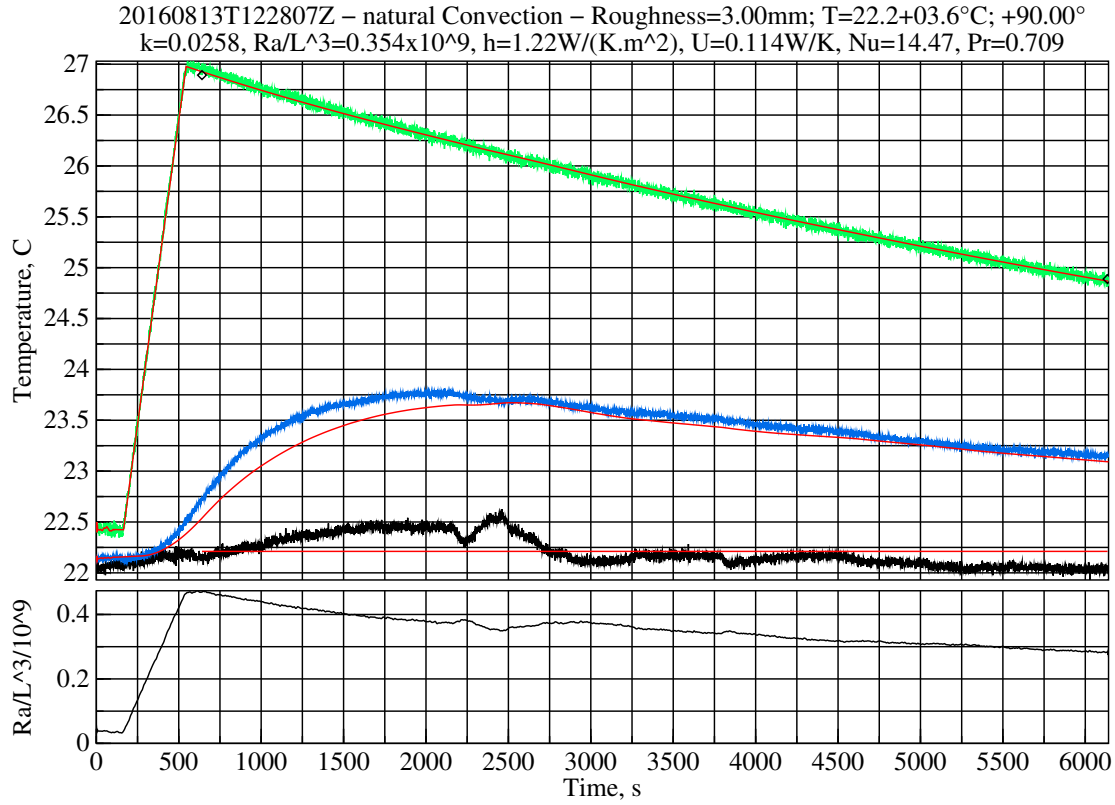
Estimated measurement uncertainties of natural convection at $\theta = 0.0$.

Symbol	Nominal	Sensitivity	Bias	Uncertainty	Component
ΔT	10.5K	+20.9%/K	0.10K	2.09%	LM35C differential
P	101kPa	+0.0007%/Pa	1.5kPa	1.03%	MPXH6115A6U air pressure
C_{pt}	4.24kJ/K	+0.044%/(J/K)	42J/K	1.86%	plate thermal capacity
C_V	1.000	−14.0%	0.100	1.40%	vertical reuptake
L_c	0.305m	+558%/m	500um	0.28%	characteristic length
D_{PIR}	25.4mm	−534%/m	1.0mm	0.53%	insulation thickness
D_g	1.00mm	−542%/m	500um	0.27%	air gap
L_m	3.57mm	+1062%/m	500um	0.53%	side metal strip width
k_{PIR}	22.2 $\frac{mW}{K \cdot m}$	+0.517%/ $\frac{mW}{K \cdot m}$	1.1 $\frac{mW}{K \cdot m}$	0.57%	PIR thermal conductivity
ϵ_{XPS}	0.515	+35.9%	0.010	0.36%	XPS emissivity
ϵ_{tp}	0.550	+43.4%	0.015	0.65%	tape emissivity
ϵ_{rs}	0.040	+155%	0.010	1.55%	test-surface emissivity
ϵ_{wt}	0.900	+54.8%	0.025	1.37%	wind-tunnel emissivity
				4.10%	combined bias uncertainty



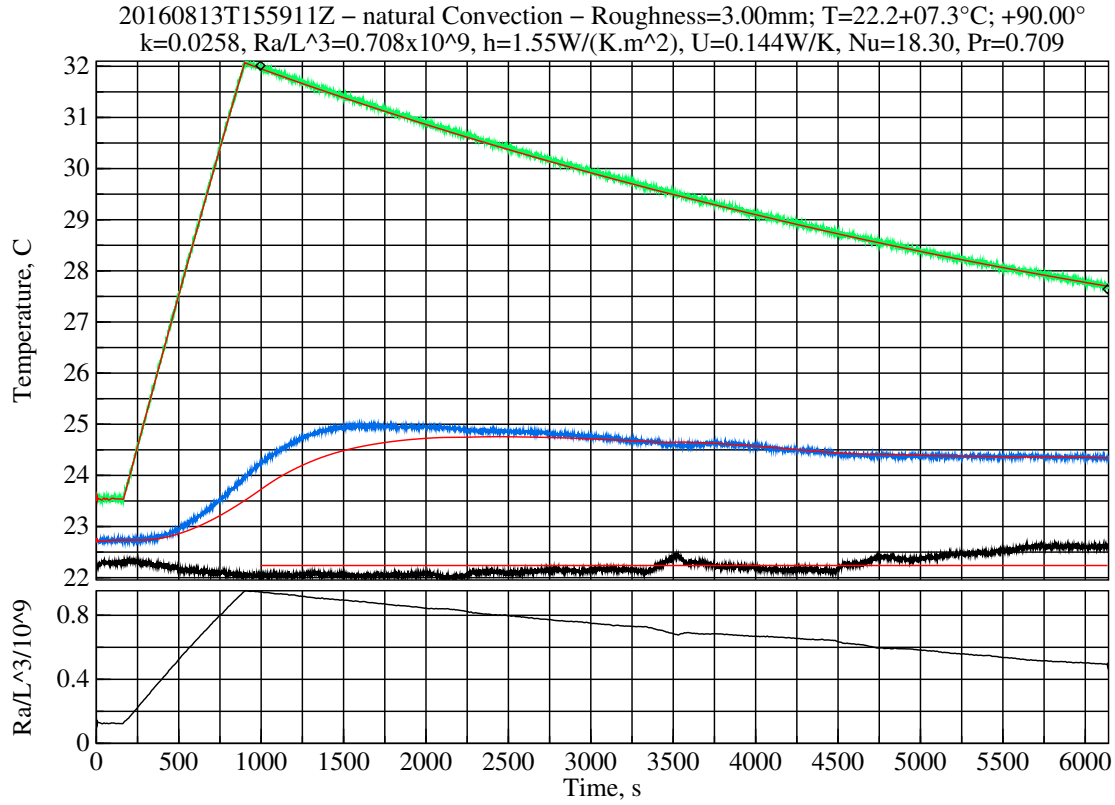
Estimated measurement uncertainties of natural convection at $\theta = 0.0$.					
Symbol	Nominal	Sensitivity	Bias	Uncertainty	Component
ΔT	14.4K	+15.0%/K	0.10K	1.50%	LM35C differential
P	101kPa	+0.0007%/Pa	1.5kPa	1.04%	MPXH6115A6U air pressure
C_{pt}	4.24kJ/K	+0.043%/(J/K)	42J/K	1.82%	plate thermal capacity
C_V	1.000	−13.7%	0.100	1.37%	vertical reuptake
L_c	0.305m	+547%/m	500um	0.27%	characteristic length
D_{PIR}	25.4mm	−505%/m	1.0mm	0.50%	insulation thickness
D_g	1.00mm	−512%/m	500um	0.26%	air gap
L_m	3.57mm	+1001%/m	500um	0.50%	side metal strip width
k_{PIR}	22.2 $\frac{mW}{K \cdot m}$	+0.488%/ $\frac{mW}{K \cdot m}$	1.1 $\frac{mW}{K \cdot m}$	0.54%	PIR thermal conductivity
ϵ_{XPS}	0.515	+33.6%	0.010	0.34%	XPS emissivity
ϵ_{tp}	0.550	+40.6%	0.015	0.61%	tape emissivity
ϵ_{rs}	0.040	+147%	0.010	1.47%	test-surface emissivity
ϵ_{wt}	0.900	+51.3%	0.025	1.28%	wind-tunnel emissivity
				3.71%	combined bias uncertainty





Estimated measurement uncertainties of natural convection at $\theta = 90.0$.

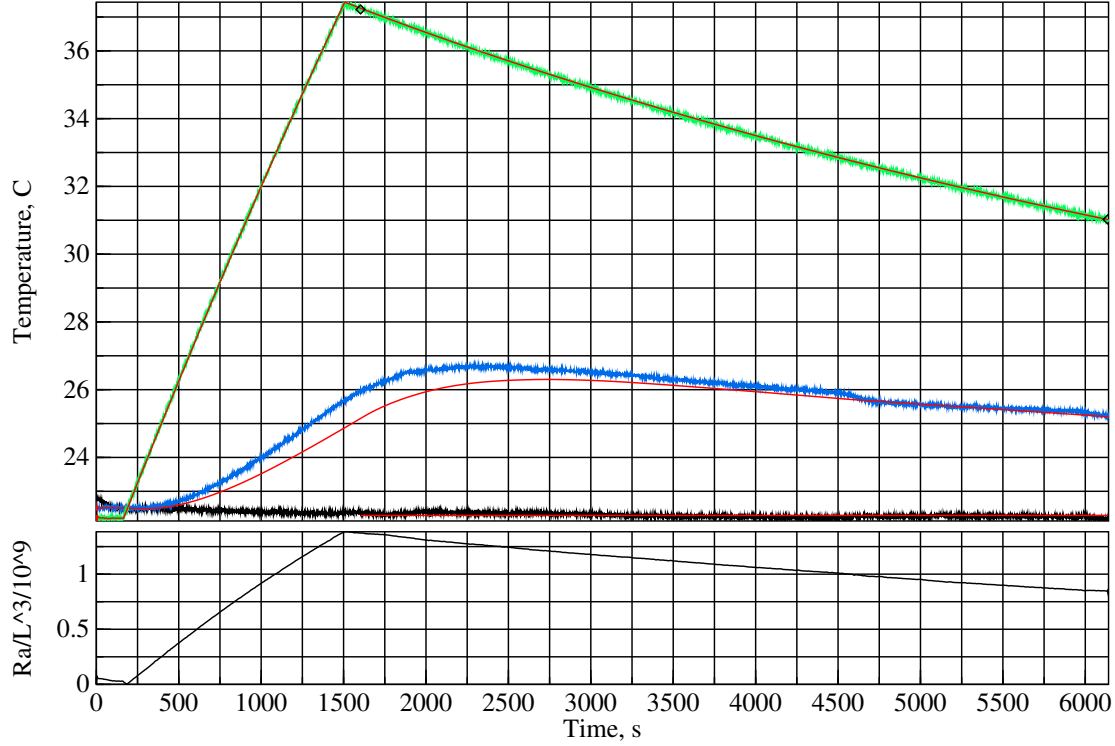
Symbol	Nominal	Sensitivity	Bias	Uncertainty	Component
T	297K	+0.827%/K	0.50K	0.41%	LM35C temperature sensor
ΔT	3.59K	+123%/K	0.10K	12.27%	LM35C differential
T_{bb}	295K	+0.889%/K	0.50K	0.44%	radiative temperature
P	101kPa	+0.0008%/Pa	1.5kPa	1.18%	MPXH6115A6U air pressure
C_{pt}	4.69kJ/K	+0.085%/(J/K)	47J/K	4.01%	plate thermal capacity
L_c	0.305m	+1225%/m	500um	0.61%	characteristic length
L_w	0.305m	+419%/m	500um	0.21%	plate width
D_{PIR}	25.4mm	−1006%/m	1.0mm	1.01%	insulation thickness
D_g	1.00mm	−1020%/m	500um	0.51%	air gap
L_m	3.57mm	+3040%/m	500um	1.52%	side metal strip width
k_{PIR}	22.2 $\frac{mW}{K \cdot m}$	+0.973%/ $\frac{mW}{K \cdot m}$	1.1 $\frac{mW}{K \cdot m}$	1.08%	PIR thermal conductivity
ϵ_{XPS}	0.515	+97.1%	0.010	0.97%	XPS emissivity
ϵ_{tp}	0.890	+117%	0.015	1.75%	tape emissivity
Ω_{tp}	0.540	+79.1%	0.020	1.58%	tape coverage
ϵ_{rs}	0.040	+408%	0.010	4.08%	test-surface emissivity
ϵ_b	0.190	+35.6%	0.020	0.71%	back emissivity
ϵ_{wt}	0.900	+197%	0.025	4.91%	wind-tunnel emissivity
θ	90.0°	−1.03%/°	0.50°	0.51%	plate angle
				14.89%	combined bias uncertainty



Estimated measurement uncertainties of natural convection at $\theta = 90.0$.

Symbol	Nominal	Sensitivity	Bias	Uncertainty	Component
T	299K	+0.697%/K	0.50K	0.35%	LM35C temperature sensor
ΔT	7.35K	+57.5%/K	0.10K	5.75%	LM35C differential
T_{bb}	295K	+0.768%/K	0.50K	0.38%	radiative temperature
P	101kPa	+0.0008%/Pa	1.5kPa	1.24%	MPXH6115A6U air pressure
C_{pt}	4.69kJ/K	+0.081%/(J/K)	47J/K	3.80%	plate thermal capacity
L_c	0.305m	+1163%/m	500um	0.58%	characteristic length
L_w	0.305m	+407%/m	500um	0.20%	plate width
D_{PIR}	25.4mm	−933%/m	1.0mm	0.93%	insulation thickness
D_g	1.00mm	−946%/m	500um	0.47%	air gap
L_m	3.57mm	+2747%/m	500um	1.37%	side metal strip width
k_{PIR}	22.2 $\frac{mW}{K \cdot m}$	+0.902%/ $\frac{mW}{K \cdot m}$	1.1 $\frac{mW}{K \cdot m}$	1.00%	PIR thermal conductivity
ϵ_{XPS}	0.515	+84.7%	0.010	0.85%	XPS emissivity
ϵ_{tp}	0.890	+102%	0.015	1.53%	tape emissivity
Ω_{tp}	0.540	+69.1%	0.020	1.38%	tape coverage
ϵ_{rs}	0.040	+365%	0.010	3.65%	test-surface emissivity
ϵ_b	0.190	+26.8%	0.020	0.54%	back emissivity
ϵ_{wt}	0.900	+171%	0.025	4.28%	wind-tunnel emissivity
θ	90.0°	−1.04%/°	0.50°	0.52%	plate angle
				9.53%	combined bias uncertainty

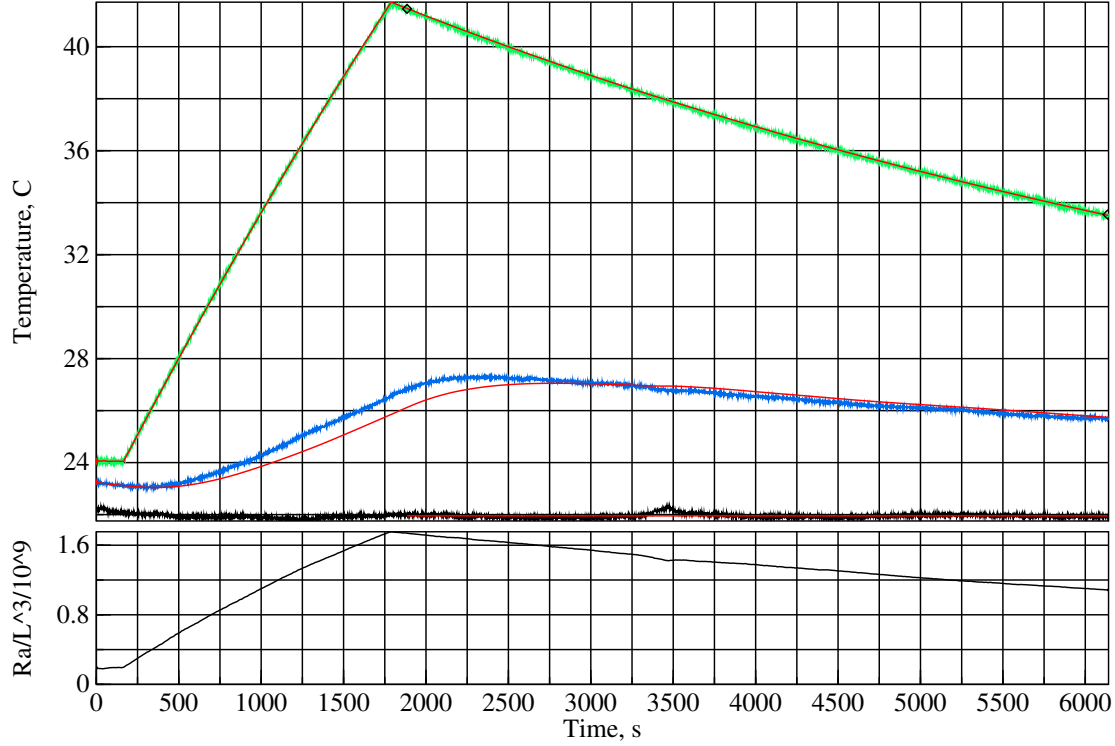
20160910T190723Z – natural Convection – Roughness=3.00mm; T=22.3+11.5°C; +90.00°
k=0.0258, Ra/L^3=1.085x10^9, h=1.65W/(K.m^2), U=0.154W/K, Nu=19.56, Pr=0.709



Estimated measurement uncertainties of natural convection at $\theta = 90.0$.

Symbol	Nominal	Sensitivity	Bias	Uncertainty	Component
T	301K	+0.632%/K	0.50K	0.32%	LM35C temperature sensor
ΔT	11.5K	+35.9%/K	0.10K	3.59%	LM35C differential
T_{bb}	296K	+0.704%/K	0.50K	0.35%	radiative temperature
P	101kPa	+0.0008%/Pa	1.5kPa	1.27%	MPXH6115A6U air pressure
C_{pt}	4.69kJ/K	+0.079%/(J/K)	47J/K	3.70%	plate thermal capacity
L_c	0.305m	+1135%/m	500um	0.57%	characteristic length
L_w	0.305m	+401%/m	500um	0.20%	plate width
D_{PIR}	25.4mm	-893%/m	1.0mm	0.89%	insulation thickness
D_g	1.00mm	-906%/m	500um	0.45%	air gap
L_m	3.57mm	+2607%/m	500um	1.30%	side metal strip width
k_{PIR}	22.2 $\frac{mW}{K \cdot m}$	+0.863%/ $\frac{mW}{K \cdot m}$	1.1 $\frac{mW}{K \cdot m}$	0.96%	PIR thermal conductivity
ϵ_{XPS}	0.515	+78.8%	0.010	0.79%	XPS emissivity
ϵ_{tp}	0.890	+95.2%	0.015	1.43%	tape emissivity
Ω_{tp}	0.540	+64.2%	0.020	1.28%	tape coverage
ϵ_{rs}	0.040	+343%	0.010	3.43%	test-surface emissivity
ϵ_b	0.190	+22.2%	0.020	0.44%	back emissivity
ϵ_{wt}	0.900	+159%	0.025	3.98%	wind-tunnel emissivity
θ	90.0°	-1.05%/°	0.50°	0.53%	plate angle
				8.05%	combined bias uncertainty

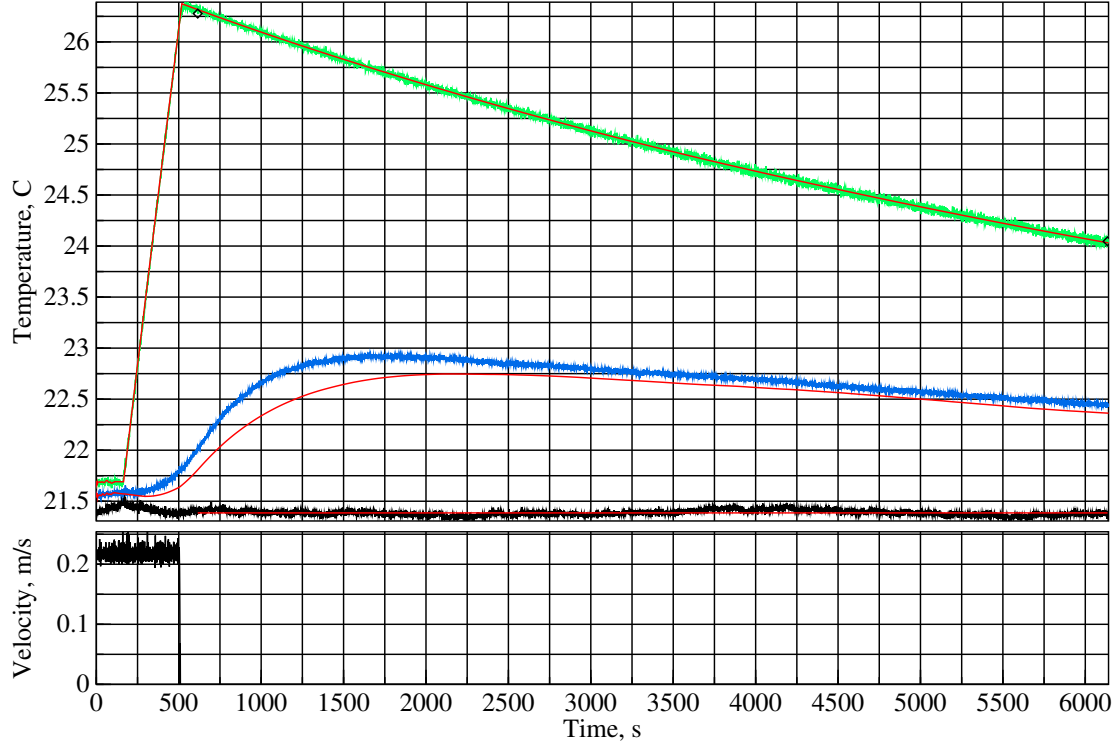
20160813T022215Z – natural Convection – Roughness=3.00mm; T=22.0+15.1°C; +90.00°
k=0.0258, Ra/L^3=1.385x10^9, h=1.63W/(K.m^2), U=0.152W/K, Nu=19.30, Pr=0.709



Estimated measurement uncertainties of natural convection at $\theta = 90.0$.

Symbol	Nominal	Sensitivity	Bias	Uncertainty	Component
T	303K	+0.602%/K	0.50K	0.30%	LM35C temperature sensor
ΔT	15.1K	+27.1%/K	0.10K	2.71%	LM35C differential
T_{bb}	295K	+0.670%/K	0.50K	0.34%	radiative temperature
P	100kPa	+0.0009%/Pa	1.5kPa	1.29%	MPXH6115A6U air pressure
C_{pt}	4.69kJ/K	+0.078%/(J/K)	47J/K	3.65%	plate thermal capacity
L_c	0.305m	+1121%/m	500um	0.56%	characteristic length
D_{PIR}	25.4mm	-871%/m	1.0mm	0.87%	insulation thickness
D_g	1.00mm	-883%/m	500um	0.44%	air gap
L_m	3.57mm	+2534%/m	500um	1.27%	side metal strip width
k_{PIR}	22.2 $\frac{mW}{K \cdot m}$	+0.842%/ $\frac{mW}{K \cdot m}$	1.1 $\frac{mW}{K \cdot m}$	0.93%	PIR thermal conductivity
ϵ_{XPS}	0.515	+75.6%	0.010	0.76%	XPS emissivity
ϵ_{tp}	0.890	+91.5%	0.015	1.37%	tape emissivity
Ω_{tp}	0.540	+61.7%	0.020	1.23%	tape coverage
ϵ_{rs}	0.040	+332%	0.010	3.32%	test-surface emissivity
ϵ_b	0.190	+19.8%	0.020	0.40%	back emissivity
ϵ_{wt}	0.900	+153%	0.025	3.82%	wind-tunnel emissivity
θ	90.0°	-1.06%/°	0.50°	0.53%	plate angle
				7.51%	combined bias uncertainty

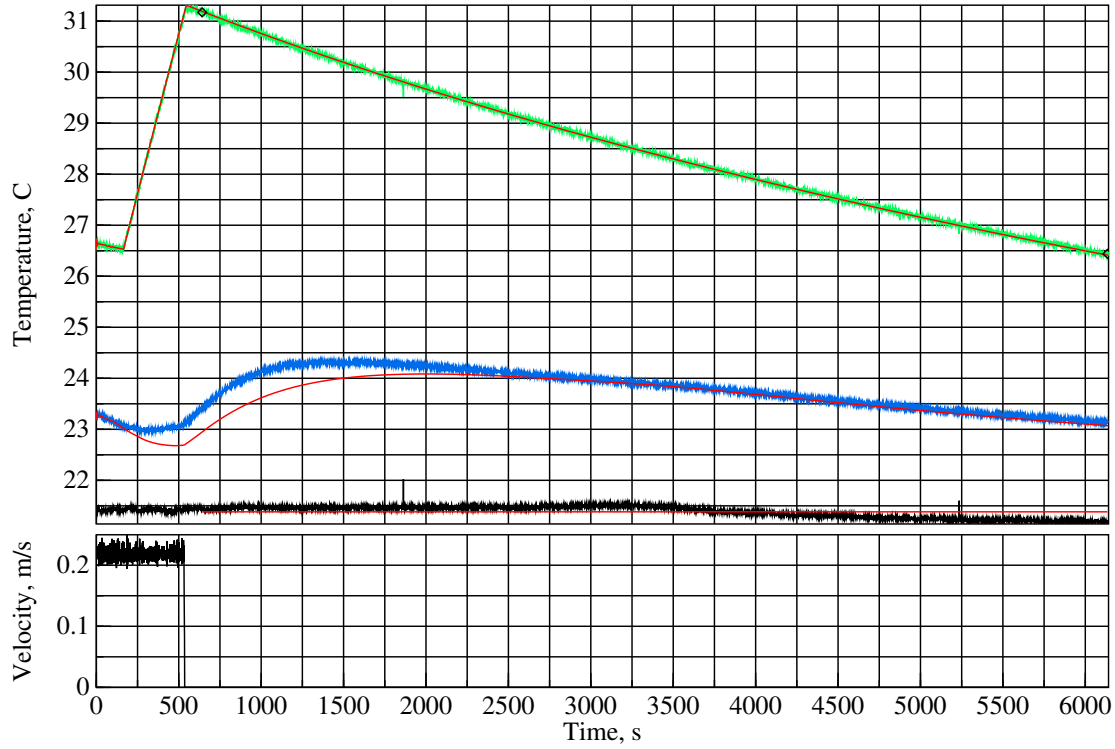
20220702T122846Z – natural Convection – Roughness=1.04mm; T=21.4+03.7°C; +90.00°
k=0.0257, Ra/L^3=0.363x10^9, h=1.24W/(K.m^2), U=0.115W/K, Nu=14.72, Pr=0.710



Estimated measurement uncertainties of natural convection at $\theta = 90.0$.

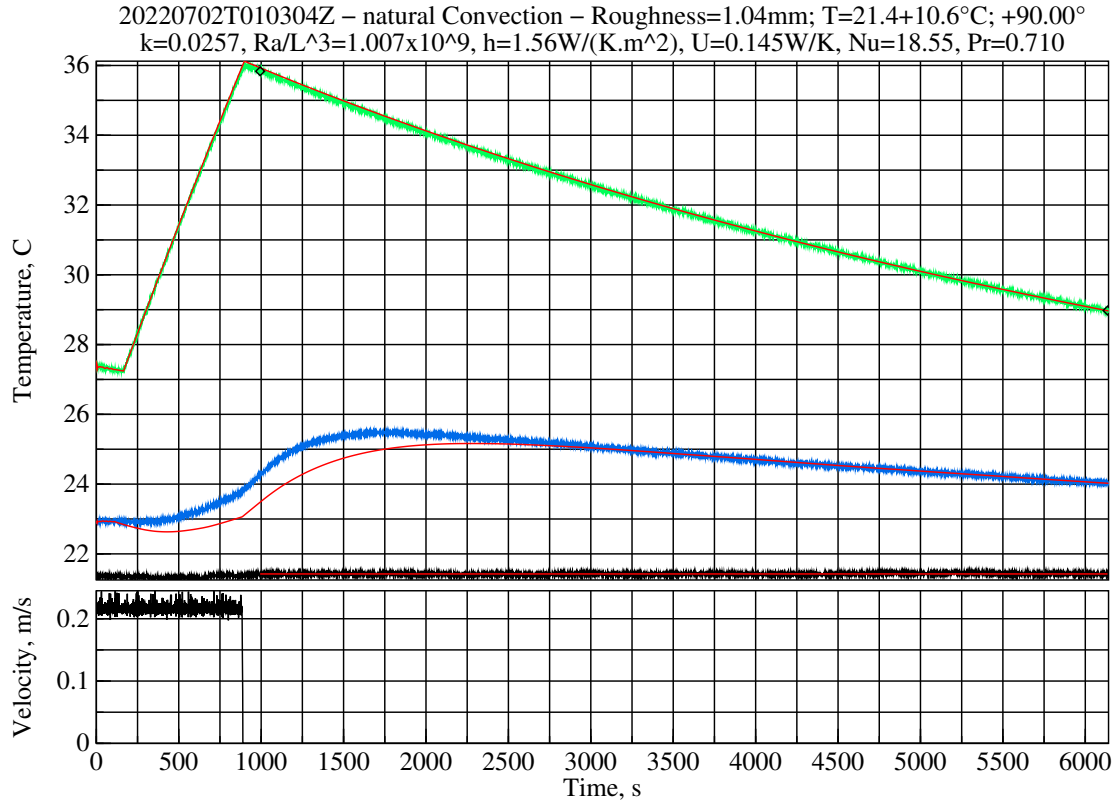
Symbol	Nominal	Sensitivity	Bias	Uncertainty	Component
T	296K	+0.831%/K	0.50K	0.42%	LM35C temperature sensor
ΔT	3.65K	+118%/K	0.10K	11.80%	LM35C differential
T_{bb}	295K	+0.890%/K	0.50K	0.45%	radiative temperature
P	100kPa	+0.0008%/Pa	1.5kPa	1.13%	MPXH6115A6U air pressure
C_{pt}	4.24kJ/K	+0.093%/(J/K)	42J/K	3.93%	plate thermal capacity
L_c	0.305m	+1199%/m	500um	0.60%	characteristic length
L_w	0.305m	+418%/m	500um	0.21%	plate width
D_{PIR}	25.4mm	−1003%/m	1.0mm	1.00%	insulation thickness
D_g	1.00mm	−1017%/m	500um	0.51%	air gap
L_m	3.57mm	+2994%/m	500um	1.50%	side metal strip width
k_{PIR}	22.2 $\frac{mW}{K \cdot m}$	+0.970%/ $\frac{mW}{K \cdot m}$	1.1 $\frac{mW}{K \cdot m}$	1.08%	PIR thermal conductivity
ϵ_{XPS}	0.515	+97.1%	0.010	0.97%	XPS emissivity
ϵ_{tp}	0.890	+116%	0.015	1.75%	tape emissivity
Ω_{tp}	0.540	+79.2%	0.020	1.58%	tape coverage
ϵ_{rs}	0.040	+405%	0.010	4.05%	test-surface emissivity
ϵ_b	0.190	+35.3%	0.020	0.71%	back emissivity
ϵ_{wt}	0.900	+196%	0.025	4.91%	wind-tunnel emissivity
θ	90.0°	−0.957%/°	0.50°	0.48%	plate angle
				14.46%	combined bias uncertainty

20220702T033704Z – natural Convection – Roughness=1.04mm; T=21.4+07.1°C; +90.00°
k=0.0257, Ra/L^3=0.695x10^9, h=1.41W/(K.m^2), U=0.131W/K, Nu=16.70, Pr=0.710



Estimated measurement uncertainties of natural convection at $\theta = 90.0$.

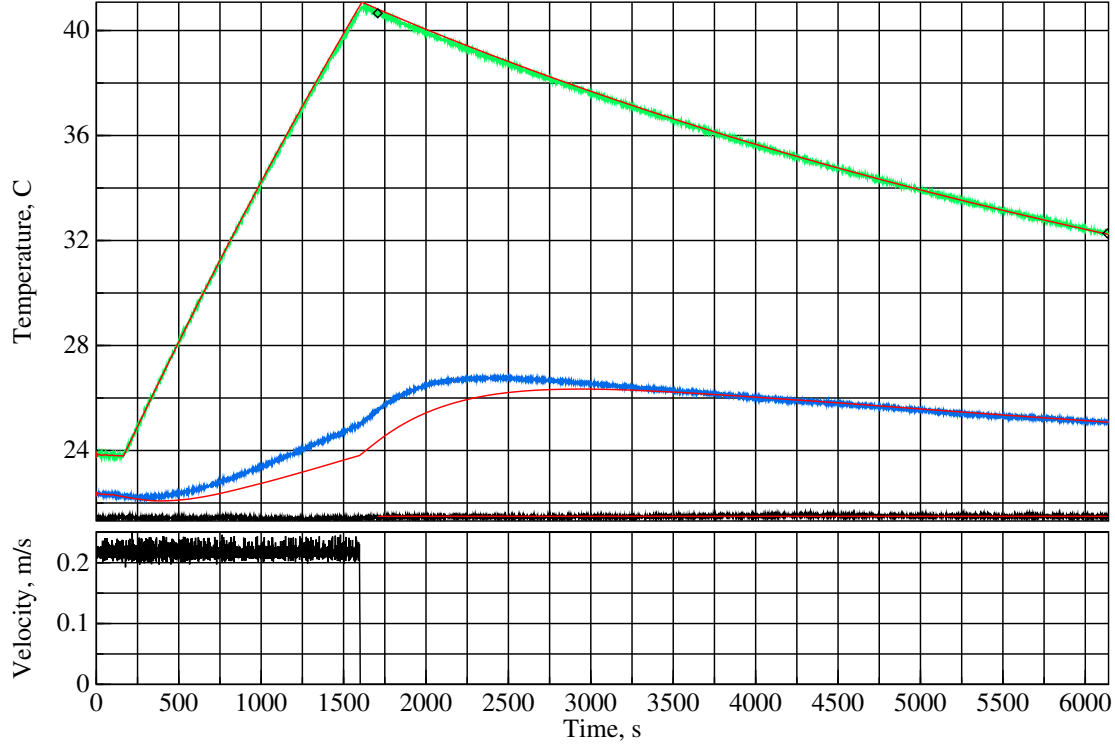
Symbol	Nominal	Sensitivity	Bias	Uncertainty	Component
T	298K	+0.711%/K	0.50K	0.36%	LM35C temperature sensor
ΔT	7.15K	+57.8%/K	0.10K	5.78%	LM35C differential
T_{bb}	295K	+0.776%/K	0.50K	0.39%	radiative temperature
P	100kPa	+0.0008%/Pa	1.5kPa	1.18%	MPXH6115A6U air pressure
C_{pt}	4.24kJ/K	+0.088%/(J/K)	42J/K	3.73%	plate thermal capacity
L_c	0.305m	+1140%/m	500um	0.57%	characteristic length
L_w	0.305m	+407%/m	500um	0.20%	plate width
D_{PIR}	25.4mm	−935%/m	1.0mm	0.93%	insulation thickness
D_g	1.00mm	−948%/m	500um	0.47%	air gap
L_m	3.57mm	+2720%/m	500um	1.36%	side metal strip width
k_{PIR}	22.2 $\frac{mW}{K \cdot m}$	+0.904%/ $\frac{mW}{K \cdot m}$	1.1 $\frac{mW}{K \cdot m}$	1.00%	PIR thermal conductivity
ϵ_{XPS}	0.515	+85.6%	0.010	0.86%	XPS emissivity
ϵ_{tp}	0.890	+103%	0.015	1.55%	tape emissivity
Ω_{tp}	0.540	+69.8%	0.020	1.40%	tape coverage
ϵ_{rs}	0.040	+364%	0.010	3.64%	test-surface emissivity
ϵ_b	0.190	+27.0%	0.020	0.54%	back emissivity
ϵ_{wt}	0.900	+173%	0.025	4.32%	wind-tunnel emissivity
θ	90.0°	−0.967%/°	0.50°	0.48%	plate angle
				9.53%	combined bias uncertainty



Estimated measurement uncertainties of natural convection at $\theta = 90.0$.

Symbol	Nominal	Sensitivity	Bias	Uncertainty	Component
T	300K	+0.654%/K	0.50K	0.33%	LM35C temperature sensor
ΔT	10.6K	+38.3%/K	0.10K	3.83%	LM35C differential
T_{bb}	294K	+0.720%/K	0.50K	0.36%	radiative temperature
P	100kPa	+0.0008%/Pa	1.5kPa	1.20%	MPXH6115A6U air pressure
C_{pt}	4.24kJ/K	+0.086%/(J/K)	42J/K	3.64%	plate thermal capacity
L_c	0.305m	+1113%/m	500um	0.56%	characteristic length
L_w	0.305m	+402%/m	500um	0.20%	plate width
D_{PIR}	25.4mm	−900%/m	1.0mm	0.90%	insulation thickness
D_g	1.00mm	−912%/m	500um	0.46%	air gap
L_m	3.57mm	+2592%/m	500um	1.30%	side metal strip width
k_{PIR}	22.2 $\frac{mW}{K \cdot m}$	+0.870%/ $\frac{mW}{K \cdot m}$	1.1 $\frac{mW}{K \cdot m}$	0.97%	PIR thermal conductivity
ϵ_{XPS}	0.515	+80.2%	0.010	0.80%	XPS emissivity
ϵ_{tp}	0.890	+96.7%	0.015	1.45%	tape emissivity
Ω_{tp}	0.540	+65.4%	0.020	1.31%	tape coverage
ϵ_{rs}	0.040	+344%	0.010	3.44%	test-surface emissivity
ϵ_b	0.190	+22.9%	0.020	0.46%	back emissivity
ϵ_{wt}	0.900	+162%	0.025	4.04%	wind-tunnel emissivity
θ	90.0°	−0.974%/°	0.50°	0.49%	plate angle
				8.17%	combined bias uncertainty

20220702T142221Z – natural Convection – Roughness=1.04mm; T=21.5+14.5°C; +90.00°
k=0.0257, Ra/L^3=1.346x10^9, h=1.55W/(K.m^2), U=0.144W/K, Nu=18.39, Pr=0.710



Estimated measurement uncertainties of natural convection at $\theta = 90.0$.

Symbol	Nominal	Sensitivity	Bias	Uncertainty	Component
T	302K	+0.617%/K	0.50K	0.31%	LM35C temperature sensor
ΔT	14.5K	+27.6%/K	0.10K	2.76%	LM35C differential
T_{bb}	295K	+0.681%/K	0.50K	0.34%	radiative temperature
P	100kPa	+0.0008%/Pa	1.5kPa	1.22%	MPXH6115A6U air pressure
C_{pt}	4.24kJ/K	+0.084%/(J/K)	42J/K	3.58%	plate thermal capacity
L_c	0.305m	+1097%/m	500um	0.55%	characteristic length
D_{PIR}	25.4mm	−874%/m	1.0mm	0.87%	insulation thickness
D_g	1.00mm	−886%/m	500um	0.44%	air gap
L_m	3.57mm	+2513%/m	500um	1.26%	side metal strip width
k_{PIR}	22.2 $\frac{mW}{K \cdot m}$	+0.845%/ $\frac{mW}{K \cdot m}$	1.1 $\frac{mW}{K \cdot m}$	0.94%	PIR thermal conductivity
ϵ_{XPS}	0.515	+76.8%	0.010	0.77%	XPS emissivity
ϵ_{tp}	0.890	+92.7%	0.015	1.39%	tape emissivity
Ω_{tp}	0.540	+62.6%	0.020	1.25%	tape coverage
ϵ_{rs}	0.040	+332%	0.010	3.32%	test-surface emissivity
ϵ_b	0.190	+20.1%	0.020	0.40%	back emissivity
ϵ_{wt}	0.900	+155%	0.025	3.87%	wind-tunnel emissivity
θ	90.0°	−0.981%/°	0.50°	0.49%	plate angle
				7.51%	combined bias uncertainty